Aerotecnica Missili & Spazio
https://doi.org/10.1007/s42496-020-00046-2

ORIGINAL ARTICLE

Optimal Two- and Three-Dimensional Earth–Moon Orbit Transfers

E. M. Leonardi[1] · **M. Pontani**[2]

Received: 19 December 2019 / Revised: 18 April 2020 / Accepted: 5 May 2020

Abstract
The determination of minimum-propellant-consumption trajectories represents a crucial issue for the purpose of planning robotic and human missions to the Moon in the near future. This work addresses the problem of identifying minimum-fuel orbit transfers from a specified low Earth orbit (LEO) to a low Moon orbit (LMO), under the assumption of employing high-thrust propulsion. The problem at hand is solved in the dynamical framework of the circular restricted three-body problem. First, the optimal two-dimensional LEO-to-LMO transfer is determined. Second, three-dimensional transfers are considered, in a dynamical model that includes the Cassini's laws of lunar motion. The propellant consumption associated with three-dimensional transfers turns out to be relatively insensitive to the final orbit inclination and exceeds only marginally the value of the globally optimal two-dimensional orbit transfer.

Keywords Earth–Moon missions · Circular restricted three-body problem · Lunar orbit dynamics · Spacecraft trajectory optimization

1 Introduction

In recent years, lunar missions are attracting an increasing interest, in the clear perspective of planning and completing robotic and human missions in the near future. In this context, identifying minimum-propellant-consumption paths represents a crucial issue.

Early studies on Earth–Moon transfers date back to the 60s. Clarke [1] proved that the use of parking orbits is more convenient than direct launch toward the Moon, with reference to mission flexibility and propellant expenditure. Miele [2] stated the theorem of optimal mirror trajectories in the Earth–Moon system in 1960, whereas Miner and Andrus [3] analyzed a rather articulated Earth–Moon mission using optimal control theory. Most recently, Miele and Mancuso [4] considered the problem of optimizing Earth–Moon paths using high-thrust propulsion, with special focus on transfer durations of a few days. They identified optimal two-dimensional trajectories from a prescribed low Earth orbit to some low-altitude lunar orbits. A similar problem was investigated by Bolt and Meiss [5] and Schroer and Ott [6], without the preceding restriction on the time of flight. Their analysis pointed out that chaotic motion in the Earth–Moon system is advantageous for the purpose of reducing the overall propellant budget, at the price of increasing considerably the time of flight. Most recently, Quarta and Mengali [7] proposed an analytic (approximate) approach that allows fast evaluation of the overall delta-v budget for optimal Earth–Moon planar transfers. While the previous investigations assumed the use of a high-thrust propulsion system, different and often more exotic options have been recently investigated for Earth–Moon missions. In the 90s, Belbruno proposed the use of weak stability boundaries for the recovery of the Japanese Hiten spacecraft [8], whereas, in recent years, several works have been devoted to Earth–Moon mission analysis using space manifold dynamics (e.g., Refs. 9 and 10, to name a few). Further interesting mission profiles were proven to be feasible if low-thrust propulsion is used, although the time of flight for similar scenarios is usually large. With this regard, relevant contributions are due to Herman and Conway [11], Bonnard and Caillau [12], Bonnard et al. [13], Kluever and Pierson [14, 15], and Kluever [16].

✉ E. M. Leonardi
e.leonardi@hotmail.it

M. Pontani
mauro.pontani@uniroma1.it

[1] Faculty of Civil and Industrial Engineering, Sapienza University of Rome, via Eudossiana 18, 00184 Rome, Italy

[2] Department of Astronautical, Electrical, and Energy Engineering, Sapienza University of Rome, via Salaria 851, 00138 Rome, Italy

Published online: 29 May 2020

Most studies employed the circular restricted three-body problem [17] as an accurate model for orbital motion under the simultaneous gravitational attraction of Earth and Moon, referred to as the primaries henceforth. In fact, this dynamical framework is rather accurate for preliminary mission analysis, aimed at identifying feasible options to accomplish the mission objectives. Nevertheless, in subsequent phases of mission design, the use of a higher-fidelity dynamical model (including orbit eccentricity of the primaries and the gravitational pull due to the Sun) is inevitable.

The present work is aimed at identifying minimum-fuel two- and three-dimensional orbit transfers from a specified low Earth orbit (LEO) to a low Moon orbit (LMO), under the assumption of employing high-thrust propulsion. The impulsive thrust approximation is adopted to model short-duration powered arcs. The problem at hand is solved in the dynamical framework of the circular restricted three-body problem, which guarantees more satisfactory accuracy in preliminary mission analysis with respect to the patched conic approximation. In fact, although it is sufficiently accurate in obtaining the first (outbound) velocity variation, for Earth–Moon missions the patched conics approximation is relatively inaccurate in estimating the periselenium altitude and the trajectory orientation relative to the Moon [18].

Specifically, this research has the following objectives: (a) formulate the optimal, two-dimensional orbit transfer problem from LEO to LMO in terms of two unknown parameters; (b) identify all the two-dimensional, short-duration feasible transfers from LEO to LMO; (c) find the globally optimal transfer with either clockwise or counterclockwise arrival at LMO; (d) formulate the optimal, three-dimensional orbit transfer problem involving two specified, non-coplanar orbits (at Earth and Moon), in terms of three unknown parameters, in a dynamical framework that includes also the Cassini's laws of lunar motion; (e) identify the globally optimal solutions for different cases, associated with distinct inclinations of the final lunar orbit. Numerical optimization for three-dimensional transfers utilizes a heuristic approach, i.e., a particular implementation of the particle swarm algorithm. This method is chosen, because it is extremely simple to program and was already employed successfully in the past for solving a variety of space trajectory optimization problems [19–23], without requiring any assumption on differentiability of the objective function of interest.

2 The Circular Restricted Three-Body Problem

In the circular restricted three-body problem (CR3BP), two primary bodies (i.e., Earth and Moon in this study) describe counterclockwise circular orbits around the center of mass of the system, with constant angular speed $\omega = \sqrt{G\left(m_{\mathrm{E}} + m_{\mathrm{M}}\right)/R_{\mathrm{EM}}^3}$ [17], where G is the universal gravitation constant, R_{EM} is the constant distance between the two primaries; whereas m_{E} and m_{M} represent the masses of Earth and Moon, respectively. They attract a third body (the spacecraft) without being attracted by it. This means that the masses m_{E}, m_{M}, and m fulfill the inequalities $m_{\mathrm{E}} > m_{\mathrm{M}} >> m \approx 0$. Moreover, canonical units are employed, i.e., the time unit (TU) and the distance unit (DU) defined as 1 DU $= R_{\mathrm{EM}}$ and 1 TU $= \omega^{-1}$. For the Earth–Moon system 1 TU $= 375{,}190$ s and 1 DU $= 384{,}400$ km. Moreover, the parameter $\mu := m_{\mathrm{M}}/\left(m_{\mathrm{M}} + m_{\mathrm{E}}\right)$ $(= 0.012155$ for the system at hand) is introduced, and the gravitational parameters of the two primaries can be written as $\mu_{\mathrm{E}} = 1 - \mu$ and $\mu_{\mathrm{M}} = \mu$ (in $\mathrm{DU}^3/\mathrm{TU}^2$). Their position along the x-axis is given by $x_{\mathrm{E}} = -\mu$ and $x_{\mathrm{M}} = (1 - \mu)$ (DU).

The synodic reference frame is associated with unit vectors $\left(\hat{\imath}, \hat{\jmath}, \hat{k}\right)$, centered at the barycenter of the Earth–Moon system. Axis $\hat{\imath}$ corresponds to the x-axis and points toward the line that connects Earth and Moon at all times, whereas $\hat{k}$ is aligned with their orbital angular momentum. As a result, the Earth and Moon positions lie along the x-axis, and the synodic frame rotates with the same angular rate of the Earth–Moon system. In this rotating frame, the spacecraft is subject to the following dynamics equations:

$$\ddot{x} - 2\omega\dot{y} = \frac{\partial U}{\partial x},\ \ddot{y} + 2\omega\dot{x} = \frac{\partial U}{\partial y},\ \ddot{z} = \frac{\partial U}{\partial z},$$
$$U := \frac{\omega\left(x^2 + y^2\right)}{2} + \frac{\mu_{\mathrm{M}}}{\sigma} + \frac{\mu_{\mathrm{E}}}{\rho}, \tag{1}$$

where (x,y,z) are the position coordinates in the synodic frame, whereas σ and ρ denote the instantaneous spacecraft distance from the center of Moon and Earth, respectively. An inertial frame, aligned with the right-hand sequence of unit vectors $\left(\hat{c}_1, \hat{c}_2, \hat{c}_3\right)$, is defined such that $\left(\hat{c}_1, \hat{c}_2, \hat{c}_3\right) \equiv \left(\hat{\imath}, \hat{\jmath}, \hat{k}\right)$ at a reference time, set to 0. This definition allows the components of the inertial velocity $\boldsymbol{v}$ along $\left(\hat{\imath}, \hat{\jmath}, \hat{k}\right)$ to be expressed as

$$V_x = \dot{x} - \omega y,\ V_y = \dot{y} + \omega x,\ V_z = \dot{z}, \tag{2}$$

Moreover, in the CR3BP an integral exists [17], i.e., the Jacobi integral, whose expression is

$$C = 2U - \left(\dot{x}^2 + \dot{y}^2 + \dot{z}^2\right). \tag{3}$$

If the Jacobi integral equals $C_1 (= 3.1883\ \mathrm{DU}^2/\mathrm{TU}^2)$, then the zero velocity curves contain the interior collinear libration point. This means that $C = C_1$ represents a limit for feasibility of the transfer from the Earth to the Moon [17], and the minimum initial speed is $v_{\min} = \sqrt{2U\left(x_0, y_0, z_0\right) - C_1}$.

3 Optimal Two-Dimensional Earth–Moon Transfers

This section is devoted to identifying the optimal transfer from a circular LEO to a circular coplanar LMO, with altitudes of 463 km and 100 km, respectively. The LEO–LMO orbit transfer problem is investigated under the following assumptions:

- the spacecraft trajectory lies entirely on the Moon orbital plane;
- the third body perturbations in LEO and LMO are neglected;
- the transfer trajectory includes two impulsive changes of velocity:
  - a tangential velocity change $\Delta \boldsymbol{v}_{LEO}$ for translunar orbit injection, and
  - a second velocity change $\Delta \boldsymbol{v}_{LMO}$ for insertion into the desired LMO.

The optimization problem consists of minimizing the total velocity variation,

$$J = \Delta v_{\mathrm{LEO}} + \Delta v_{\mathrm{LMO}},$$
$$\text{where } \Delta v_{\mathrm{LEO}} = \left|\Delta \mathbf{v}_{\mathrm{LEO}}\right| \text{ and } \Delta v_{\mathrm{LMO}} = \left|\Delta \mathbf{v}_{\mathrm{LMO}}\right|. \tag{4}$$

3.1 Formulation of the Problem

This subsection demonstrates that two parameters are sufficient to identify a two-dimensional LEO–LMO orbit transfer, i.e., (a) magnitude of the first velocity change Δv_{LEO}, and (b) the angle δ that separates $\hat{\imath}$ from the position vector of the spacecraft relative to the Earth center at the initial time. After the first velocity change, the coordinates of the spacecraft position and velocity (relative to the synodic frame) are

$$x_0 = x_{\mathrm{E}} + R_{\mathrm{LEO}} \cos\delta \quad \text{and} \quad y_0 = R_{\mathrm{LEO}} sin\delta; \tag{5}$$

$$\dot{x}_0^+ = \left(\omega R_{\mathrm{LEO}} - v_0\right) \sin\delta \text{ and}$$
$$\dot{y}_0^+ = \left(v_0 - \omega R_{\mathrm{LEO}}\right)\cos\delta$$
$$\left(v_0 = \sqrt{\mu_{\mathrm{E}}/R_{\mathrm{LEO}}} + \Delta v_{\mathrm{LEO}}\right). \tag{6}$$

These values represent the initial conditions for Eq. (1), written in the form of four first-order differential equations and governing the translunar transfer arc. Intersection with the final LMO occurs at t_f, when the space craft has coordinates $\left(x_f, y_f\right)$ and position relative to the Moon denoted with $\boldsymbol{r}_{f,M}$. The angle θ between $\boldsymbol{r}_{f,M}$ and $\hat{\imath}$ is given by

$$\sin\theta = \frac{y_{\mathrm{f}}}{R_{\mathrm{LMO}}} \text{ and } \cos\theta = \frac{x_{\mathrm{f}} - x_{\mathrm{M}}}{R_{\mathrm{LMO}}}. \tag{7}$$

The desired velocity components $\left(\dot{x}_f^+, \dot{y}_f^+\right)$ after the second velocity change correspond to the velocity along a circular LMO,

$$\dot{x}_{\mathrm{f}}^+ = \mp\sqrt{\mu_{\mathrm{M}}/R_{\mathrm{LMO}}}\sin\theta + \omega y_{\mathrm{f}} \text{ and}$$
$$\dot{y}_{\mathrm{f}}^+ = \pm\sqrt{\mu_{\mathrm{M}}/R_{\mathrm{LMO}}}\cos\theta - \omega\left(x_{\mathrm{f}} - x_{\mathrm{M}}\right). \tag{8}$$

where for the symbols $\mp$ and $\pm$, the first and second option correspond, respectively, to counterclockwise and clockwise lunar orbits. Therefore, if $\left(\dot{x}_{\mathrm{f}}^-, \dot{y}_{\mathrm{f}}^-\right)$ denote the components before the second velocity change, then $\Delta v_{\mathrm{LMO}} = \sqrt{\left(\dot{x}_{\mathrm{f}}^+ - \dot{x}_{\mathrm{f}}^-\right)^2 + \left(\dot{y}_{\mathrm{f}}^+ - \dot{y}_{\mathrm{f}}^-\right)^2}$.

In the end, the Earth–Moon transfer is proven to be identified by a pair of parameters, i.e., $\left(\Delta v_{\mathrm{LEO}}, \delta\right)$. They are sought in the following intervals:

$$3.025\frac{\mathrm{km}}{\mathrm{s}} \le \Delta v_{\mathrm{LEO}} \le 3.162\frac{\mathrm{km}}{\mathrm{s}} \quad 0 \le \delta \le 2\pi, \tag{9}$$

where the lower bound for Δv_{LEO} is obtained using the condition $C = C_1$ (cf. Sect. 2); while, the upper bound corresponds to the escape velocity from the Earth gravitational field.

3.2 Method of Solution and Numerical Results

A graphical study has been performed to identify the feasibility ranges for the pair of unknown parameters (Δv_{LEO} ,δ). The related locus in the (Δv_{LEO},δ)-plane collects all the trajectories that intersect the desired final orbit within 10 days after departure. Figure 1 illustrates this locus and the contour plot of the objective function. From inspection of Fig. 1, it is apparent that the region where the objective function assumes higher values (highlighted in yellow) is surrounded by two neighboring regions with lower values (in blue). Each of these two regions corresponds to a different direction of the angular momentum of the LMO, that is, counterclockwise or clockwise orbits, associated, respectively, with the lower and upper bounds. The fact that the optimal paths lie on the boundary of feasible trajectories implies that injection into LMO is performed tangentially, analogously to what occurs for the Hohmann transfer in the restricted two-body problem.

As a final step, for either clockwise or counterclockwise LMO, the globally optimal solution, corresponding to the minimum propellant consumption, is determined using the native Matlab function *fminsearch*. This represents a routine for local optimization, and exhibits excellent convergence for the cases at hand, because satisfactory guess solutions are provided by inspection of Fig. 1. The two optimal solutions are located around the lowest values of Δv_{LEO} and the

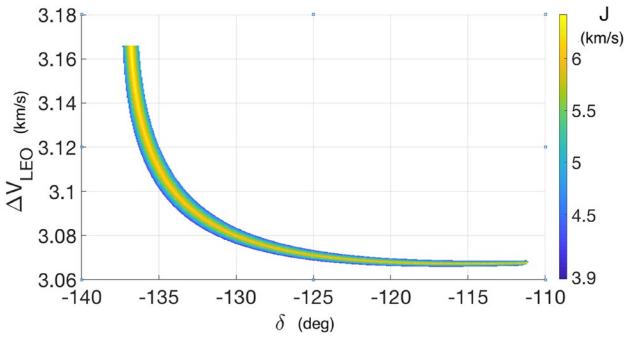

Fig. 1 Contour plot of the objective function $J(\Delta v_{LEO}, \delta)$

highest values of δ. It is worth remarking that in this region, close values of the objective function correspond to relatively different values of δ. This reduced sensitivity of the objective function, emphasized also in Ref. 7, has practical implications, because different directions can be chosen at departure, with modest effects on the overall propellant consumption. Table 1 collects the results of the optimization process. These are extremely close to those found by Miele and Mancuso [4] in terms of Δv_{LEO}, although they slightly differ in terms of departure angle δ. However, these results are slightly more accurate than those of Ref. 4, where the authors identified the center of the Earth with the center of the entire system. Moreover, these numerical results are in excellent agreement with the analytical formulas presented in Ref. 7 (also aimed at evaluating the overall delta-v in relation to alternative transfer options). Figure 2 portrays the transfer trajectory for both counterclockwise and clockwise arrivals at LMO.

Table 1 Globally optimal two-dimensional LEO–LMO orbit transfers

	J (km/s)	Δv_{LEO} (km/s)	δ(deg)
Clockwise	3.885	3.069	− 117.52
Counterclockwise	3.878	3.066	− 117.38

4 Optimal Three-Dimensional Earth–Moon Transfers

This section addresses the determination of the optimal three-dimensional orbit transfer from an initial LEO to a final LMO, both with specified altitude and inclination. Specifically, the initial orbit has an altitude of 463 km and an inclination of 51.6 deg, whereas different final circular lunar orbits are considered, with a common altitude of 100 km and distinct inclinations. The initial altitude is identical to that assumed for planar transfers (cf. Sect. 3), to compare the results being achieved with those attained in Sect. 3. Assumptions (b) and (c) of Sect. 3 still hold; in particular, the first velocity change is again tangential to the initial velocity. The optimization problem consists again of minimizing the cost function defined in Eq. (4).

4.1 Reference Frames

As a first step, the Earth-centered inertial frame (ECI) and the Moon-centered frame (MC) are defined in relation to the heliocentric inertial frame (HCI). The latter reference system is associated with the unit vectors $(\hat{c}_1, \hat{c}_2, \hat{c}_3)$, where $\hat{c}_1$ is the vernal axis (corresponding to the intersection of the ecliptic plane with the Earth equatorial plane) and $\hat{c}_3$ points toward the Earth orbit angular momentum [24]. The ECI frame is associated with the unit vectors $\left(\hat{c}_1^{(E)}, \hat{c}_2^{(E)}, \hat{c}_3^{(E)}\right)$, where $\hat{c}_1^{(E)}$ is the vernal axis and $\hat{c}_3^{(E)}$ points toward the Earth rotation axis [24]. The ECI frame and the HCI frame are related through the ecliptic obliquity angle, δ_{E} (= 23.45 deg),

$$\left[\hat{c}_1^{(\mathrm{E})}\ \hat{c}_2^{(\mathrm{E})}\ \hat{c}_3^{(\mathrm{E})}\right]^{\mathrm{T}} = R_1(-\delta_{\mathrm{E}})\left[\hat{c}_1\ \hat{c}_2\ \hat{c}_2\right]^{\mathrm{T}}, \tag{8}$$

where the notation $R_j(\chi)$ refers to an elementary counterclockwise rotation by angle χ about axis j. According to Cassini's laws, the Moon's rotation axis $\hat{z}_{\mathrm{M}}$ is coplanar with

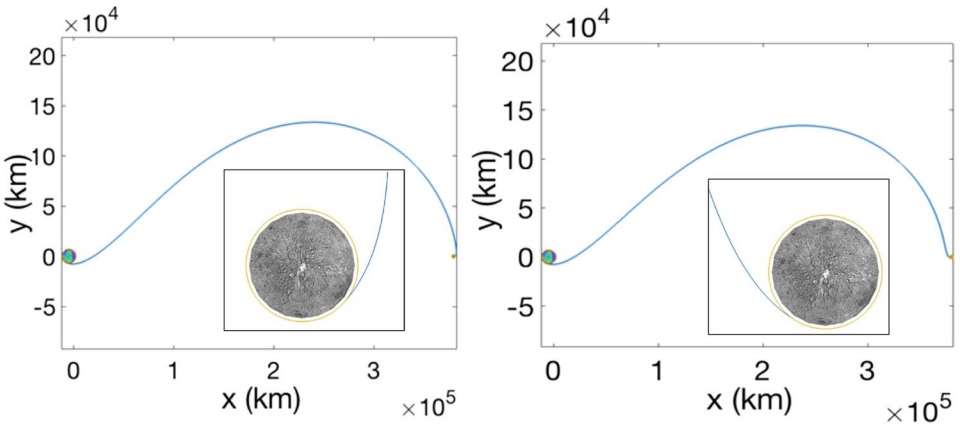

Fig. 2 Plot of the 2D trajectory in $(\hat{\imath}, \hat{\jmath}, \hat{k})$ (**a**) Clockwise LMO, (**b**) Counterclockwise LMO

the Moon's orbit angular momentum $\mathbf{h}_{\mathrm{M}}$ and the normal to the ecliptic plane $\hat{c}_3$. The two vectors $\hat{z}_{\mathrm{M}}$ and $\mathbf{h}_{\mathrm{M}}$ are located at the opposite sides of the ecliptic pole $\hat{c}_3$, and both of them are subject to clockwise precession due to the Sun, with a period of 18.6 years. Hence, axis $\hat{c}_3^{(M)}$ of the MC frame can be properly identified as the rotation axis $\hat{z}_{\mathrm{M}}$ at a reference epoch t_{ref}, $\hat{c}_3^{(\mathrm{M})} = \hat{z}_{\mathrm{M}}(t_{\mathrm{ref}})$. The remaining two axes lie in the Moon equatorial plane; by definition, $\hat{c}_1^{(\mathrm{M})}$ is coplanar with the line that connects the Earth and the Moon at t_{ref} and is directed toward the far side of the Moon. Using these definitions, the directions of unit vectors $\hat{c}_1^{(\mathrm{M})}$, $\hat{c}_2^{(\mathrm{M})}$, and $\hat{c}_3^{(\mathrm{M})}$ are inertial (although the origin of the MC frame rotates). If ψ_{M} and δ_{M} denote, respectively, the precession angle and the Moon equator obliquity (separating $\hat{c}_3^{(\mathrm{M})}$ from $\hat{c}_3$), then

$$\left[\,\hat{c}_1^{(\mathrm{M})}\;\;\hat{c}_2^{(\mathrm{M})}\;\;\hat{c}_3^{(\mathrm{M})}\,\right]^T = R_1(\delta_{\mathrm{M}})R_3\left(\psi_{\mathrm{M}}^{(\mathrm{ref})}\right)\left[\,\hat{c}_1\;\;\hat{c}_2\;\;\hat{c}_2\,\right]^{\mathrm{T}}, \tag{9}$$

where $\psi_{\mathrm{M}}^{(\mathrm{ref})}$ $(= -81.7\mathrm{deg})$ represents the precession angle at t_{ref} (set to 1 June 2029) and $\delta_{\mathrm{M}} = 1.5\mathrm{deg}$. Because the LEO–LMO transfer completes in a few days, ψ_{M} is assumed constant and equal to $\psi_{\mathrm{M}}^{(\mathrm{ref})}$. Moreover, the inertial orbital frame $\left(\widehat{N}_{\mathrm{M}}, \widehat{M}_{\mathrm{M}}, \widehat{h}_{\mathrm{M}}\right)$ can be introduced, with unit vectors $\widehat{N}_{\mathrm{M}}$ and $\widehat{h}_{\mathrm{M}}$ aligned with the ascending node and the angular momentum of the lunar orbit at t_{ref}. This frame is related to $\left(\hat{c}_1^{(\mathrm{E})}, \hat{c}_2^{(\mathrm{E})}, \hat{c}_3^{(\mathrm{E})}\right)$ through the inclination and the right ascension of the ascending node (RAAN) of the lunar orbit at t_{ref},

$$\left[\,\hat{N}_{\mathrm{M}}\;\;\hat{M}_{\mathrm{M}}\;\;\hat{h}_{\mathrm{M}}\,\right]^T = R_1(i_{\mathrm{M}})R_3(\Omega_{\mathrm{M}})\left[\,\hat{c}_1^{(\mathrm{E})}\;\;\hat{c}_2^{(\mathrm{E})}\;\;\hat{c}_3^{(\mathrm{E})}\,\right]^{\mathrm{T}}. \tag{10}$$

Finally, the synodic frame aligned with $(\hat{\imath}, \hat{\jmath}, \hat{k})$ is related to $\left(\widehat{N}_{\mathrm{M}}, \widehat{M}_{\mathrm{M}}, \widehat{h}_{\mathrm{M}}\right)$ through a single counterclockwise rotation about axis 3 by angle $\alpha := \omega(t - \bar{t})$, which means that these two frames are aligned when $t = \bar{t} + 2k\pi/\omega\,(k \in \mathbb{Z})$,

$$\left[\,\hat{\imath}\;\;\hat{\jmath}\;\;\hat{k}\,\right]^{\mathrm{T}} = R_3(\alpha)\left[\,\hat{N}_{\mathrm{M}}\;\;\hat{M}_{\mathrm{M}}\;\;\hat{h}_{\mathrm{M}}\,\right]^{\mathrm{T}}. \tag{11}$$

The symbol $\bar{t}$ denotes a generic epoch when the two frames $(\hat{\imath}, \hat{\jmath}, \hat{k})$ and $\left(\widehat{N}_{\mathrm{M}}, \widehat{M}_{\mathrm{M}}, \widehat{h}_{\mathrm{M}}\right)$ coincide. The previous definitions remove all the assumptions related to two-dimensional motion that were introduced in Sect. 3.

4.2 Formulation of the Problem

In this study, the three-dimensional LEO–LMO transfer is formulated in terms of three unknown parameters: (a) magnitude of the first velocity change Δv_{LEO}, (b) right ascension of LEO Ω_{LEO}, and (c) the initial phase angle α_i between the synodic reference frame $(\hat{\imath}, \hat{\jmath}, \hat{k})$ and the inertial frame $\left(\widehat{N}_{\mathrm{M}}, \widehat{M}_{\mathrm{M}}, \widehat{\mathrm{h}}_{M}\right)$. If t_i denotes the initial time, then $\alpha_i \equiv \omega(t_i - \bar{t})$. The initial orbit inclination is instead specified and denoted with i_{LEO}. The unit vector $\hat{h}$, associated with the spacecraft angular momentum prior to departure, can be written in terms of $(\Omega_{\mathrm{LEO}}, i_{\mathrm{LEO}})$,

$$\hat{h} = \left[\,\sin\Omega_{\mathrm{LEO}}\sin i_{\mathrm{LEO}}\;\;-\cos\Omega_{\mathrm{LEO}}\sin i_{\mathrm{LEO}}\;\;\cos i_{\mathrm{LEO}}\,\right] \left[\,\hat{c}_1^{(\mathrm{E})}\;\;\hat{c}_2^{(\mathrm{E})}\;\;\hat{c}_3^{(\mathrm{E})}\,\right]^{\mathrm{T}}. \tag{12}$$

The first tangential impulse is applied at one of the two intersection points between the Moon orbit plane and the LEO, with the intent of injecting the spacecraft into LMO at the opposite intersection point. The line that contains these two points is aligned with the unit vector

$$\hat{r}_0 = \frac{\hat{h}_{\mathrm{M}} \times \hat{h}}{\left|\hat{h}_{\mathrm{M}} \times \hat{h}\right|}. \tag{13}$$

Moreover, at departure from the Earth orbit, the local vertical local horizontal frame (LVLH) is associated with the right-hand sequence $(\hat{r}_0, \hat{\theta}_0, \hat{h})$, where

$$\hat{\theta}_0 = \hat{h} \times \hat{r}_0. \tag{14}$$

The initial values for the numerical integration of Eq. (1) can be obtained under the assumption that the initial velocity change is applied tangentially, i.e., along $\hat{\theta}_0$. As a result, if $\mathbf{v}_{\mathrm{E}}$ denotes the inertial velocity of the Earth in its motion around the Earth–Moon barycenter, then the spacecraft inertial velocity in the CR3BP right after the first velocity change is

$$\mathbf{v} = v_0\hat{\theta}_0 + \mathbf{v}_{\mathrm{E}},\ \text{where}\ v_0 = \sqrt{\mu_{\mathrm{E}}/R_{\mathrm{LEO}}} + \Delta v_{\mathrm{LEO}}\ \text{and}\ \mathbf{v}_{\mathrm{E}} = \omega x_{\mathrm{E}}\hat{\jmath}. \tag{15}$$

To provide the initial conditions for the numerical integration of Eq. (1), the previous relation must be written in the synodic frame. To do this, $\hat{\theta}_0$ is first obtained in the ECI frame using Eqs. (10) and (12)–(14). Then, Eqs. (10) and (11) are employed to project $\hat{\theta}_0$ in the synodic frame. Once the three components (V_x, V_y, V_z) of $\mathbf{v}$ along $(\hat{\imath}, \hat{\jmath}, \hat{k})$ have been identified, the initial conditions $(\dot{x}_0^+, \dot{y}_0^+, \dot{z}_0^+)$ can be found using Eq. (2). Moreover, the spacecraft position vector at departure, taken from the origin of the Earth–Moon system and denoted with $\mathbf{r}_i$, is given by

$$\mathbf{r}_i = x_{\mathrm{E}}\hat{\imath} + R_{\mathrm{LEO}}\hat{r}_0. \tag{16}$$

Using steps similar to those for $\hat{\theta}_0$, also $\hat{r}_0$ can be projected into the synodic frame $(\hat{\imath}, \hat{\jmath}, \hat{k})$, and this leads to identifying the initial conditions for the position coordinates (x_0, y_0, z_0).

The final conditions at injection correspond to intersection of the transfer arc with the sphere centered at the Moon and with radius equal to that of the final orbit. The related components in the synodic frame are denoted with $\left(x_f, y_f, z_f, \dot{x}_f^-, \dot{y}_f^-, \dot{z}_f^-\right)$. Using Eqs. (9)–(11), the position vector relative to the Moon center, $\mathbf{r}_{f,M}$, can be expressed in the MCI frame as

$$\mathbf{r}_{f,M} = \begin{bmatrix} x_f - x_M & y_f & z_f \end{bmatrix} \begin{bmatrix} \hat{\imath} & \hat{\jmath} & \hat{k} \end{bmatrix}^T = \begin{bmatrix} x_f - x_M & y_f & z_f \end{bmatrix} \boldsymbol{A}\left(\alpha_f, i_M, \Omega_M, \delta_E, \psi_M, \delta_M\right) \begin{bmatrix} \hat{c}_1^{(M)} & \hat{c}_2^{(M)} & \hat{c}_3^{(M)} \end{bmatrix}^T, \tag{17}$$

where

$$\boldsymbol{A}\left(\alpha_{\mathrm{f}}, i_{\mathrm{M}}, \Omega_{\mathrm{M}}, \delta_{\mathrm{E}}, \psi_{\mathrm{M}}, \delta_{\mathrm{M}}\right) := \mathrm{R}_3\left(\alpha_{\mathrm{f}}\right)\mathrm{R}_1\left(i_{\mathrm{M}}\right)\mathrm{R}_3\left(\Omega_{\mathrm{M}}\right)\mathrm{R}_1\left(-\delta_E\right)\mathrm{R}_3^T\left(\psi_{\mathrm{M}}^{(\mathrm{ref})}\right)\mathrm{R}_1^T\left(\delta_{\mathrm{M}}\right). \tag{18}$$

Matrix **A** is the result of several subsequent elementary rotations, $\alpha_{\mathrm{f}} = \alpha_i + \omega\Delta t$, and Δt represents the flight time. The desired orbit plane has specified inclination i_{f}, whereas its RAAN Ω_f is found by solving the equation $\mathbf{r}_{\mathrm{f,M}} \cdot \mathbf{h}_{\mathrm{f,M}} = 0$, after writing $\mathbf{h}_{\mathrm{f,M}}$ in terms of i_{f} and Ω_{f},

$$\mathbf{h}_{f,M} = \begin{bmatrix} sin\Omega_f \sin i_f & -\cos\Omega_f \sin i_f & \cos i_f \end{bmatrix} \begin{bmatrix} \hat{c}_1^{(M)} & \hat{c}_2^{(M)} & \hat{c}_3^{(M)} \end{bmatrix}^T. \tag{19}$$

Using Eqs. (17) and (19), the orthogonality condition $\mathbf{r}_{\mathrm{f,M}} \cdot \mathbf{h}_{\mathrm{f,M}} = 0$ assumes the following form:

$$a_1 \cos\Omega_{\mathrm{f}} + a_2 \sin\Omega_{\mathrm{f}} + a_3 = 0, \tag{20}$$

where the terms $a_k\,(k = 1, 2, 3)$ depend on $\left\{x_f, y_f, z_f, \alpha_f, i_M, \Omega_M, \delta_E, \psi_M, \delta_M, i_f\right\}$. In general, Eq. (20) yields two solutions, and the one associated with the lower value of the objective function is selected. Once the final orbit has been determined, the velocity components $\left(\dot{x}_{\mathrm{f}}^+, \dot{y}_{\mathrm{f}}^+, \dot{z}_{\mathrm{f}}^+\right)$ can be found using steps analogous to those described at the beginning of this section, with $\left(\hat{c}_1^{(\mathrm{M})}, \hat{c}_2^{(\mathrm{M})}, \hat{c}_3^{(\mathrm{M})}\right)$ in place of $\left(\hat{c}_1^{(\mathrm{E})}, \hat{c}_2^{(\mathrm{E})}, \hat{c}_3^{(\mathrm{E})}\right)$. Therefore, if $\left(\dot{x}_{\mathrm{f}}^-, \dot{y}_{\mathrm{f}}^-, \dot{z}_{\mathrm{f}}^-\right)$ denote the components before the second velocity change, then

$$\Delta v_{\mathrm{LMO}} = \sqrt{\left(\dot{x}_{\mathrm{f}}^+ - \dot{x}_{\mathrm{f}}^-\right)^2 + \left(\dot{y}_{\mathrm{f}}^+ - \dot{y}_{\mathrm{f}}^-\right)^2 + \left(\dot{z}_{\mathrm{f}}^+ - \dot{z}_{\mathrm{f}}^-\right)^2}. \tag{21}$$

In the end, the Earth–Moon transfer is proven to be identified by three parameters, i.e., $\left(\Delta v_{\mathrm{LEO}}, \Omega_{\mathrm{LEO}}, \alpha_i\right)$. They are sought in the following intervals:

$$\begin{aligned} &3.025\,\mathrm{km/s} \le \Delta v_{\mathrm{LEO}} \le 3.162\,\mathrm{km/s}, \\ &0 \le \Omega_{\mathrm{LEO}} \le 2\pi \quad 0 \le \alpha_i \le \pi \end{aligned} \tag{22}$$

where the lower bound for Δv_{LEO} is obtained again using the condition $C = C_1$ (cf. Sect. 2); while, the upper bound corresponds to the escape velocity from the Earth gravitational field.

4.3 Method of Solution

The particle swarm optimization (PSO) method [19] is a heuristic technique aimed at finding the optimal values of a set of unknown parameters, for a generic dynamical system. In general, unconstrained parameter optimization problems can be stated as follows: determine the optimal values of the n_P unknown parameters $\left\{\chi_1, \ldots, \chi_{n_P}\right\}$ such that the objective function is minimized. The PSO technique is a population-based method, where the population is represented by a swarm of N particles. Each particle i $(i = 1, \ldots, N)$ is associated with a position vector $\boldsymbol{\chi}(i)$ and with a velocity vector $\mathbf{w}(i)$. The position vector includes the values of the n_P unknown parameters ($n_P = 3$ for the problem at hand) ; whereas, the velocity vector determines the position update. Each particle represents a possible solution to the problem, and corresponds to a specific value of the objective function. The initial population is randomly generated by introducing N particles, whose positions and velocities are (stochastically) uniformly distributed in the respective search spaces. The expressions for position and velocity update determine the swarm evolution toward the location of the globally optimal position, which corresponds to the globally optimal solution to the problem of interest. The algorithm terminates when the maximum number of iterations N_{IT} is reached or an alternative convergence criterion is met. The position vector of the best particle is expected to contain the optimal values of the unknown parameters, which correspond to the global minimum of the objective function. The central idea underlying the method is contained in the formula for velocity updating. This formula includes three terms with stochastic weights: the first term is the so-called inertial component and for each particle is proportional to its velocity in the preceding iteration; the second component is termed the cognitive component, directed toward the personal best position, i.e., the best position experienced by the particle; and finally, the third term is the social component, directed toward the global best position, i.e., the best position yet located by any particle in the swarm. Further details on the specific implementation of PSO used in this study are provided in Ref. 19.

For the problem at hand, the particle swarm algorithm is used, with three unknown parameters $\left(\Delta v_{\mathrm{LEO}}, \alpha_i, \Omega_{\mathrm{LEO}}\right)$. The optimization is repeated with different values for the inclination of the LMO, ranging from 0 to 90 deg.

4.4 Numerical Results

The three unknown parameters $\left(\Delta v_{\mathrm{LEO}}, \Omega_{\mathrm{LEO}}, \alpha_i\right)$ are sought in the search space reported in Eq. (22), for each case associated with a prescribed value the inclination of the LMO.

From inspecting the results in Table 2, it is evident that the overall velocity change is only marginally greater than the value found for the two-dimensional transfer. Unsurprisingly, the total velocity change decreases with the inclination of the final lunar orbit. In fact, reaching lunar orbits with lower inclinations requires intercepting the Moon at

Table 2 Results for the three-dimensional LEO–LMO orbit transfer

i_{LMO} (deg)	J (km/s)	Δv_{LEO} (km/s)	Ω_{LEO} (deg)	α_i (deg)
90	3.89445	3.06812	− 12.05	121.32
80	3.89376	3.06784	− 11.44	122.42
70	3.89278	3.06750	− 12.91	119.75
60	3.89162	3.06713	− 11.15	122.48
50	3.89028	3.06677	− 12.47	119.69
40	3.88906	3.06644	− 12.60	118.78
30	3.88802	3.06616	− 12.53	117.96
20	3.88731	3.06598	− 11.32	118.89
10	3.88713	3.06593	− 12.21	115.97
0	3.88796	3.06606	− 11.59	115.16

lower latitudes, resulting in a reduced Δv_{LEO} at translunar injection. It is worth remarking that the selection of the initial optimal RAAN can take advantage of the orbit precession motion due to the Earth oblateness. Moreover, if a final polar LMO with a specific RAAN is desired, this can be achieved in three steps, i.e., (a) selecting a final orbit with lower inclination (e.g., 80 deg), (b) waiting until precession (due to Moon oblateness) changes the RAAN to the desired value, and (c) performing a final out-of-plane maneuver to change the inclination to 90 deg. Figures 3 and 4 portray two optimal LEO–LMO transfers, associated, respectively, with final lunar polar and equatorial orbits.

5 Concluding Remarks

This work addresses the problem of identifying minimum-fuel two- and three-dimensional orbit transfers from a specified low Earth orbit (LEO) to a low Moon orbit (LMO), under the assumption of employing high-thrust propulsion. The problem at hand is solved in the dynamical framework of the circular restricted three-body problem. First, the optimal two-dimensional orbit transfer from LEO to LMO is formulated in terms of two unknown parameters, and all the feasible transfers are identified. Then, the globally optimal two-impulse transfer is found, and is proven to be located at the boundary of the feasible region of the search space associated with Earth–Moon transfers. As a second step, three-dimensional transfers are considered, using a dynamical model that includes also the Cassini's laws of lunar motion. Several two-impulse optimal orbit transfers are identified, corresponding to distinct final lunar orbits. Selection of the initial optimal RAAN can benefit from precession of the orbit plane due to Earth oblateness. The propellant consumption associated with three-dimensional transfers turns out

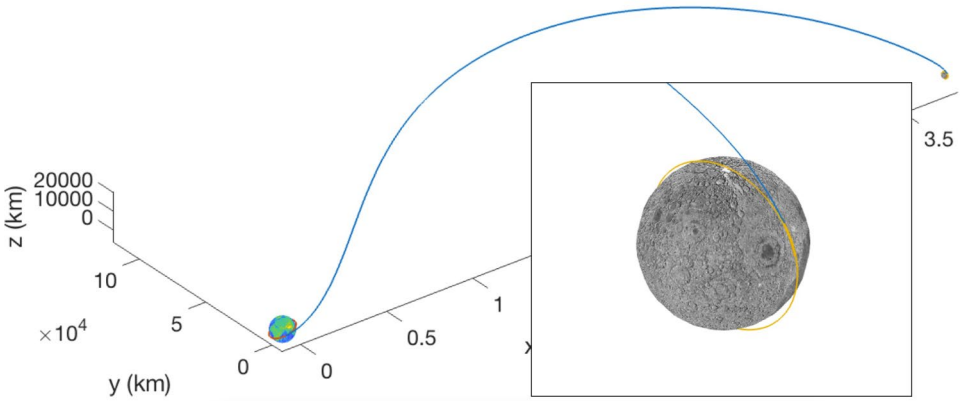

Fig. 3 Plot of the 3D trajectory in $(\hat{\imath}, \hat{\jmath}, \hat{k})$ (with arrival at polar LMO in the inset)

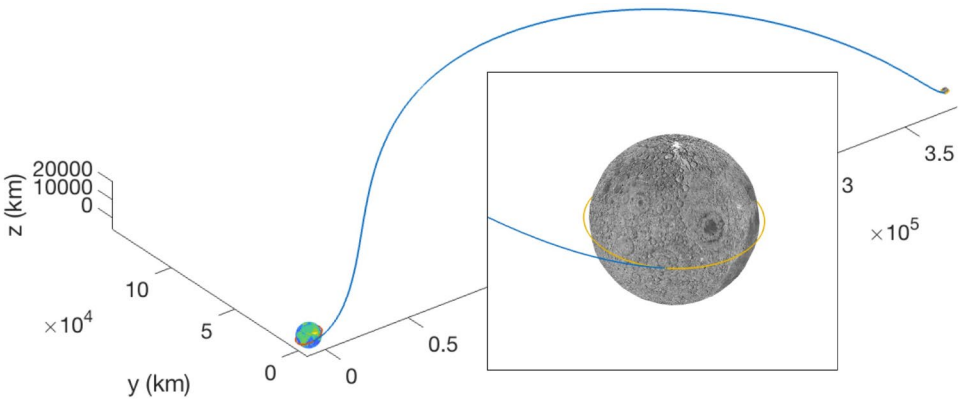

Fig. 4 Plot of the 3D trajectory in $(\hat{\imath}, \hat{\jmath}, \hat{k})$ (with arrival at equatorial LMO in the inset)

to be relatively insensitive to the final orbit inclination and exceeds only marginally the value of the globally optimal two-dimensional orbit transfer.

Compliance with ethical standards

Conflict of interest On behalf of all authors, the corresponding author states that there is no conflict of interest.

References

1. Clarke, V.C.: Design of lunar and interplanetary ascent trajectories. AIAA J. **1**(7), 1559–1567 (1963)
2. Miele. Theorem of image trajectories in the earth-moon space. Astronautica Acta, **6**(51), 225–232 (1960).
3. Miner, W.E., Andrus, J.F.: Necessary conditions for optimal lunar trajectories with discontinuous state variables and intermediate point constraints. AIAA J. **6**(11), 2154–2159 (1968)
4. Mancuso, M.S.: Optimal trajectories for earth-moon-earth flight. Acta Astronaut. **49**(2), 59–71 (2001)
5. Bollt, E.M., Meiss, J.D.: Targeting chaotic orbits to the moon through recurrence. Phys. Lett. A **204**(5–6), 373–378 (1995)
6. Schroer, C.G., Ott, E.: Targeting in hamiltonian systems that have mixed regular/chaotic phase spaces. Chaos **7**(4), 512–519 (1997)
7. Mengali, G., Quarta, A.: Optimization of biimpulsive trajectories in the earth-moon restricted three-body problem. J. Guidance Control Dyn. **28**(2), 209–216 (2005)
8. Belbruno, E.A., Miller, J.K.: Sun-peturbed earth-to-moon transfers with ballistic capture. J. Guidance Control Dyn. **16**(4), 770–775 (1993)
9. Pontani, M., Teofilatto, P.: Polyhedral representation of invariant manifolds applied to orbit transfers in the Earth-Moon system. Acta Astronaut. **119**, 218–232 (2016)
10. Ozimek, M.T., Howell, K.C.: Low-thrust transfers in the earth-moon system including applications to libration point orbits. J. Guidance Control Dyn. **33**(2), 533–549 (2010)
11. Herman, L., Conway, B.A.: Optimal, low-thrust, earth-moon orbit transfer. J Guidance Control Dyn. **21**(1), 141–147 (1998)
12. Bonnard, J.-B.C.: Riemannian metric of the averaged energy minimization problem in orbital transfer with low thrust. Ann. L'Institut Henri Poincaré **24**, 395–411 (2007)
13. Bonnard, B., Caillau, J.-B., Dujol, R.: Energy minimization of single input orbit transfer by averaging and continuation. Bull. Sci. Math. **130**, 707–719 (2006)
14. Kluever, A., Pierson, B.L.: Optimal Earth-Moon trajectories using nuclear electric propulsion. J. Guidance Control Dyn. **20**(2), 239–245 (1997)
15. Kluever, C.A., Pierson, B.L.: Optimal low-thrust three-dimensional Earth-Moon trajectories. J Guidance Control Dyn. **18**(4), 830–837 (1995)
16. Kluever, C.A.: Optimal Earth-Moon trajectories using combined chemical-electric propulsion. J Guidance Control Dyn. **20**(2), 253–258 (1997)
17. Szebehely, V.: Theory of Orbits in the Restricted Problem of Three Bodies, pp. 7–22. Academic Press, London (1967)
18. Bate, R.R., Mueller, D.D., White, J.E.: Fundamentals of Astrodynamics, p. 333. Dover, New York (1971)
19. Pontani, M., Conway, B.: Particle swarm optimization applied to space trajectories. J. Guidance Control Dyn. **33**(5), 1429–1441 (2010)
20. Pontani, M., Conway, B.A.: Optimal low-thrust orbital maneuvers via indirect swarming method. J. Optim. Theory Appl. **162**(1), 272–292 (2014)
21. Pontani, M., Conway, B.A.: Particle swarm optimization applied to impulsive orbital transfers. Acta Astronaut. **74**, 141–155 (2012)
22. Pontani, M., Ghosh, P., Conway, B.: Particle swarm optimization of multiple-burn rendezvous trajectories. J. Guidance Control Dyn. **35**(4), 1192–1207 (2012)
23. Pontani, M.: Particle swarm optimization of ascent trajectories of multistage launch vehicles. Acta Astronaut. **94**(2), 852–864 (2014)
24. Roy, E.: Orbital Motion, pp. 20–28. IOP Publishing Ltd., London (2005). **304-305**